SUPPLEMENTARY DATA

Missed cleavage opportunities by FEN1 lead to Okazaki fragment maturation via the long-flap pathway

Manal S. Zaher[1], Fahad Rashid[1,#], Bo Song[2,#], Luay I. Joudeh[1], Mohamed A. Sobhy[1], Muhammad Tehseen[1], Manju M. Hingorani[2] and Samir M. Hamdan*[1]

[1] King Abdullah University of Science and Technology, Division of Biological and Environmental Science and Engineering, Thuwal 23955, Saudi Arabia.

[2] Department of Molecular Biology and Biochemistry, Wesleyan University, Middletown, Connecticut 06459, USA

* To whom correspondence should be addressed. Tel: +966 (0) 12 808 2384; Email: samir.hamdan@kaust.edu.sa

[#] The authors wish it to be known that, in their opinion, the second and third authors should be regarded as joint Second Authors

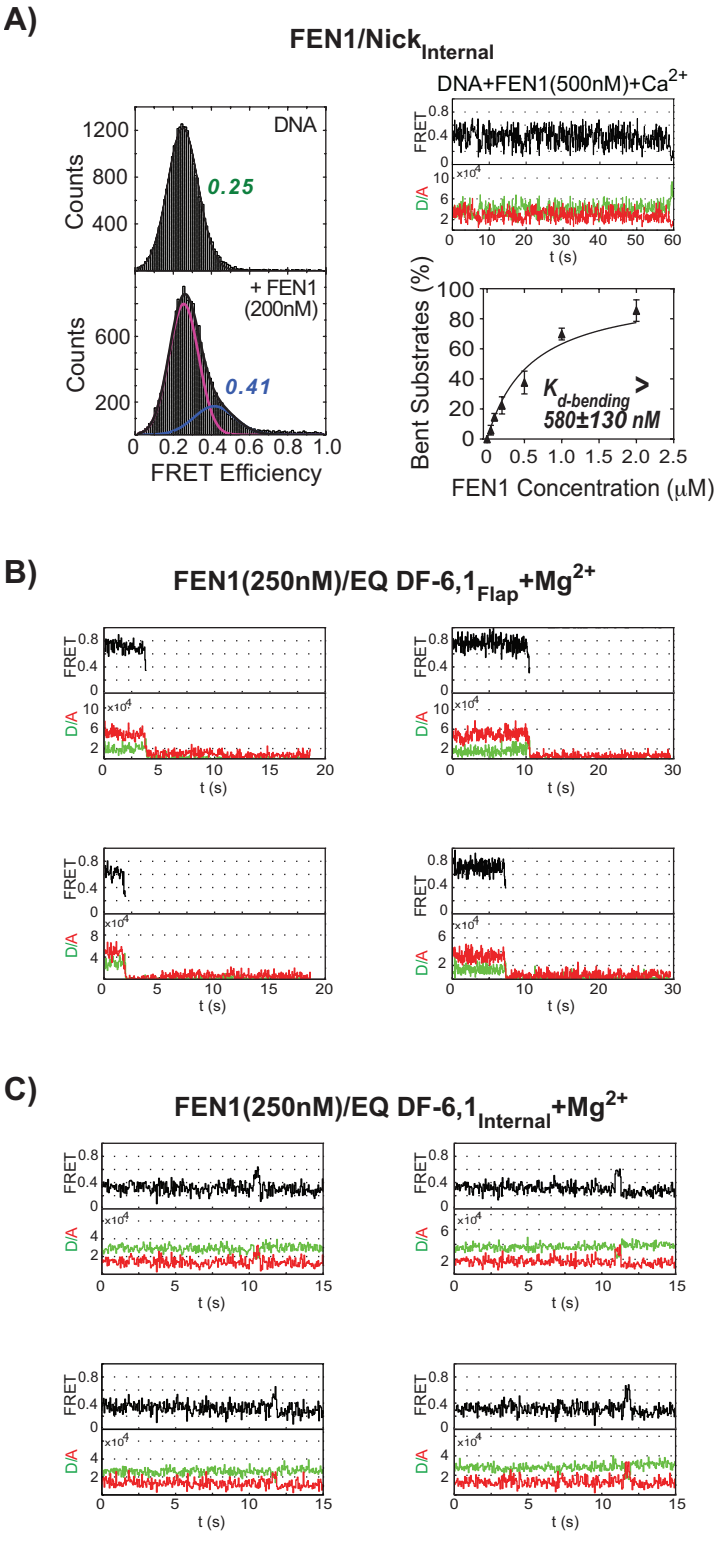

Supplementary Figure 1. (A) smFRET bending efficiency of FEN1 on Nick$_{Internal}$. Left panel shows smFRET histograms of Nick$_{Internal}$ DNA-only (top) with a single peak centered around 0.25 and upon addition of 200 nM FEN1 (bottom) with two peaks. The two peaks are merged and the centers are shifted. If the unbent peak (highlighted in magenta) center is fixed at 0.25, then the bent peak (highlighted in blue) appears to be centered around 0.41. Increasing the binding affinity of FEN1 to Nick$_{Internal}$ by lowering KCl from 100 mM to 40 mM, removes the averaging effect and clearly shows that the FRET state of Nick$_{Internal}$ upon binding FEN1 is similar to that of DF-6,1$_{Internal}$ (E ~0.5; see Supplementary Figure 2A). Right

top: a representative single molecule time trace of $Nick_{Internal}$ upon addition of 500 nM FEN1. The time trace shows fast transitions between unbent (0.25) and bent (0.52) states. The transitions appear to be much faster than the acquisition temporal resolution of 100 ms. Right bottom: an isotherm of the percentage of bent substrate (%) versus FEN1 concentration (nM) fitted to a one-site binding model with Bmax≤100 yields $K_{d\text{-}bending}$. As described for Figure 7E, the $K_{d\text{-}bending}$ of FEN1 on $Nick_{Internal}$ is a lower estimate. This is due to the averaging effect caused by the fast transitions seen in the time traces and, consequently, merging and shifting of the peak centers in histograms, which complicates fitting and estimation of the % bent substrate at each concentration and thus explicit determination of $K_{d\text{-}bending}$. **(B)** Representative single molecule time traces showing cleavage of EQ DF-6,1_{Flap} using the flap-labeling smFRET cleavage assay as in Figure 3A. **(C)** Representative single molecule time traces showing cleavage of EQ DF-6,$1_{Internal}$ using the internal-labeling smFRET cleavage assay. FEN1 bends and cleaves the substrate almost always within the first bending event, as in Figure 3C.

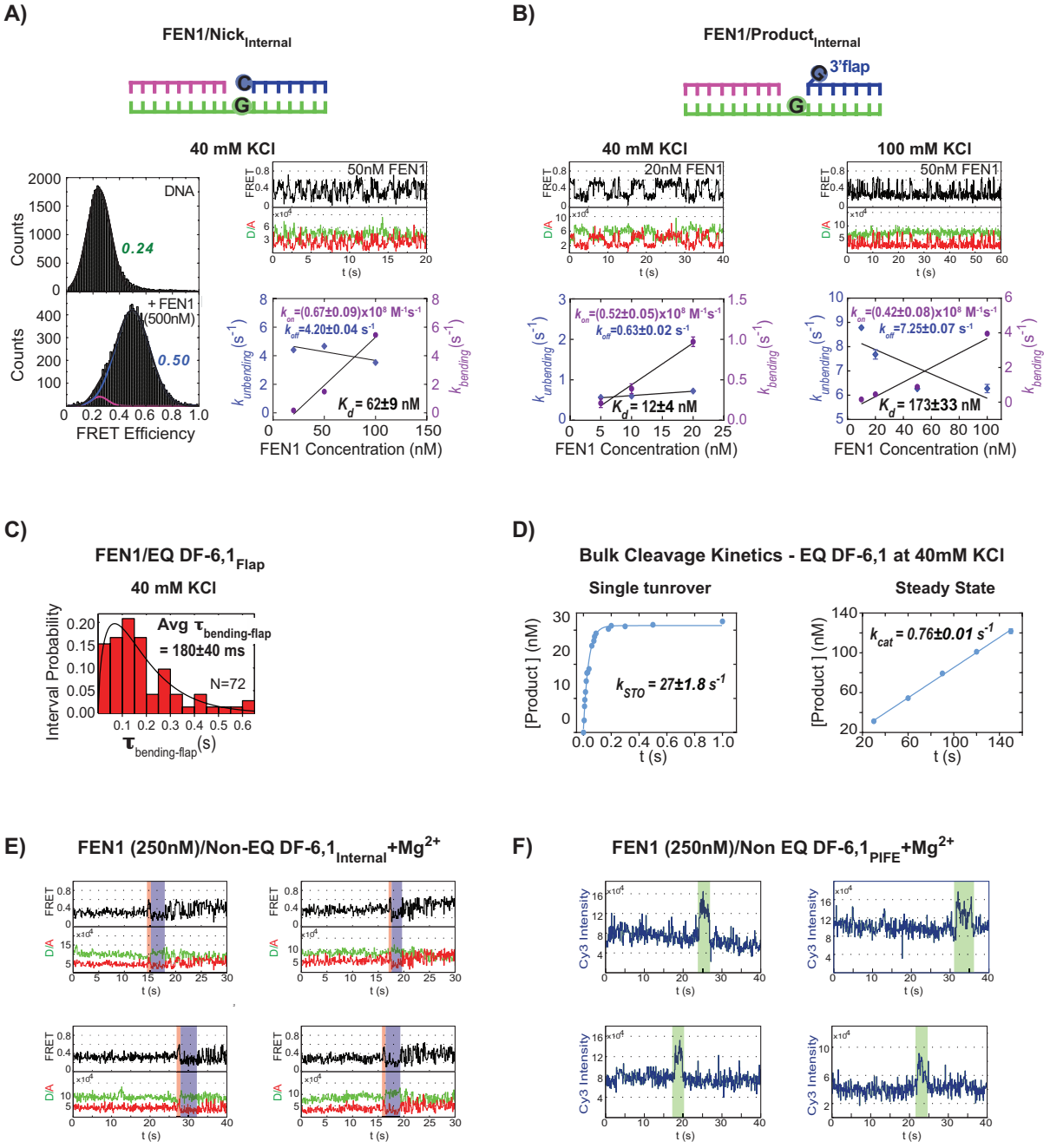

Supplementary Figure 2. (A) smFRET bending kinetics of $Nick_{Internal}$ by FEN1 at 40 mM KCl in the presence of Ca^{2+}. Top: a schematic showing the $Nick_{Internal}$ structure. Left: smFRET histograms of $Nick_{Internal}$ alone and upon addition of 500 nM FEN1. Unbent DNA-alone peak (shown in magenta) is centered around 0.24 and bent peak (in blue) is centered around 0.5. Right Top: a representative single molecule time trace of $Nick_{Internal}$ upon addition of 50 nM FEN1. The trace shows transitions between unbent (0.25) and bent (0.52) states. Right Bottom: a graph of $k_{bending}$ (s^{-1}) and $k_{unbending}$ (s^{-1}) versus FEN1 concentrations (nM). The values of $k_{bending}$, $k_{unbending}$, $k_{off\text{-}unbending}$, $k_{on\text{-}bending}$ and $K_{d\text{-}bending}$ are determined as described for Figure 2B. **(B)** smFRET bending kinetics of $Product_{Internal}$ by FEN1 in the presence of Ca^{2+}. Top: a schematic showing the $Product_{Internal}$ structure with a fixed non-equilibrated 1 nt 3' flap mimicking the cleavage product of a Non EQ DF substrate. Left: bending kinetics of $Product_{Internal}$ at 40 mM KCl, with the middle panel showing a single molecule time trace of $Product_{Internal}$ upon addition of 20 nM FEN1 exhibiting dynamic behavior, and the bottom panel showing the association and dissociation rate constants as described in (A). Right: bending kinetics of $Product_{Internal}$ at 100 mM KCl. At higher salt, $Product_{Internal}$ displays faster

transitions with a significantly elevated $k_{off\text{-}unbending}$, and hence $K_{d\text{-}bending}$. However, $k_{on\text{-}bending}$ is not influenced by salt concentration. **(C)** smFRET cleavage of EQ DF-6,1$_{Flap}$ by FEN1 at 40 mM KCl. Distribution of the dwell times spent in the bent state ($\tau_{bending\text{-}flap}$) for N=72 cleavage events. The average $\tau_{bending\text{-}flap}$ at 40 mM KCl is comparable to that obtained at 100 mM KCl (Figure 3A). The cleavage reaction was performed at 50 ms temporal resolution. **(D)** Bulk cleavage kinetics of EQ-DF6,1 by FEN1 at 40 mM KCl. Single turnover (left) and steady state (right) kinetics were measured and fit as described in Figure 3B, yielding k_{STO} and k_{cat}, respectively. k_{STO} is slightly faster and k_{cat} is slightly slower than the rates obtained at 100 mM KCl (Figure 3B). **(E)** Representative time traces of smFRET cleavage of Non EQ DF6,1$_{Internal}$ by FEN1 at 40 mM KCl. The traces show similar behavior to that shown in Figure 4B. **(F)** Representative time traces of smPIFE cleavage of Non EQ DF-6,1$_{PIFE}$ by FEN1 at 100 mM KCl. The traces show similar behavior to that shown in Figure 4C.

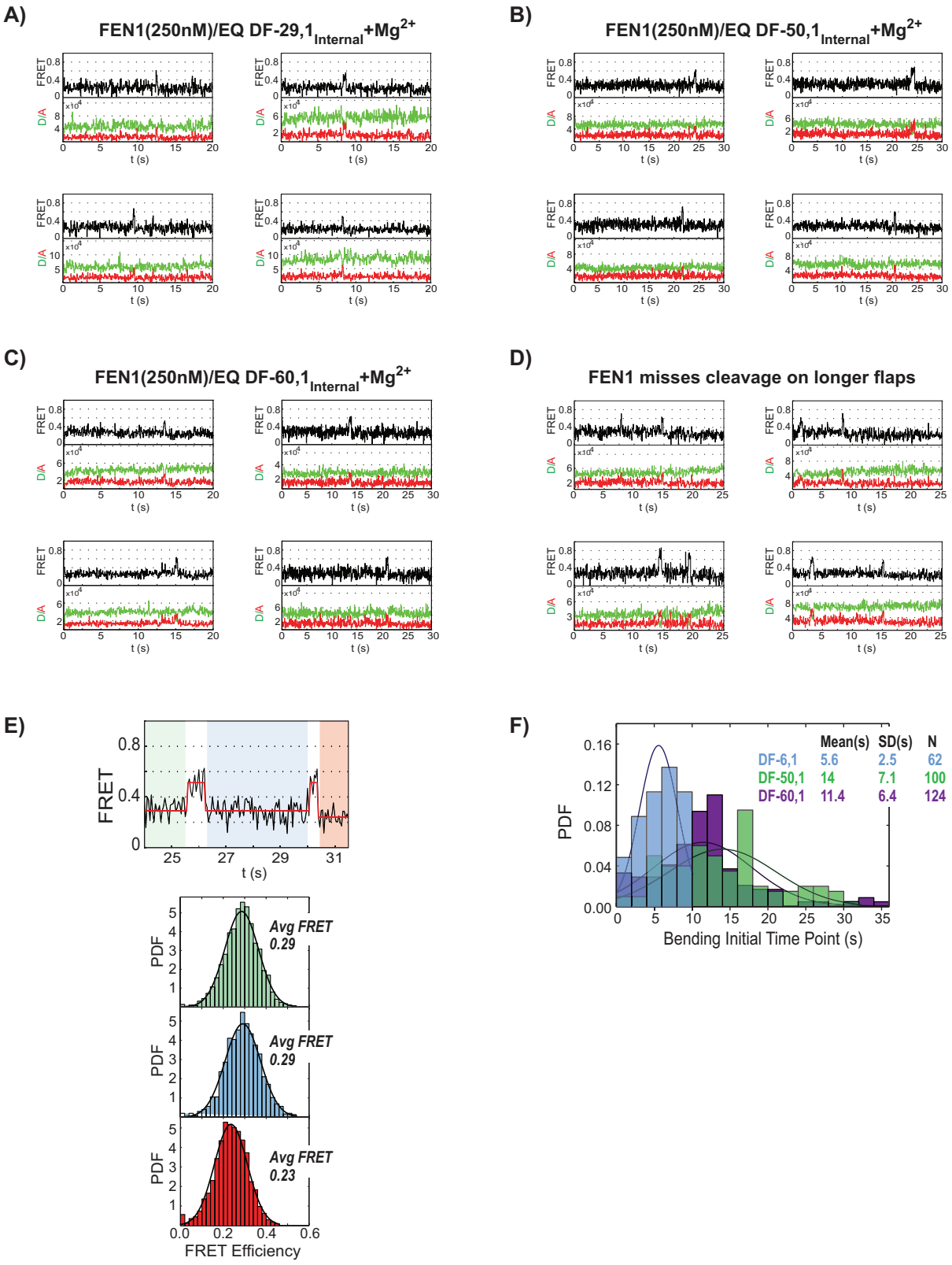

Supplementary Figure 3. (A) Representative time traces showing cleavage of EQ DF-29,1$_{Internal}$ wherein FEN1 cleaves the substrate within the first bending event as in Figure 6A. **(B)** Representative time traces showing cleavage of EQ DF-50,1$_{Internal}$ wherein FEN1 cleaves the substrate within the first bending event as in Figure 6B. **(C)** Representative time traces showing cleavage of EQ DF-60,1$_{Internal}$ wherein FEN1 cleaves the substrate within the first bending event as in Figure 6C. **(D)** Representative time traces showing cleavage of long DF

substrates with missed opportunities as shown in Figure 6D. **(E)** Assignment of a bending event as missed cleavage or actual cleavage. Time traces that exhibit multiple bending events in EQ-DF-50,1$_{Interanl}$ cleavage reaction (N=15) were considered for further quantification of the unbent FRET state. As shown on the representative time trace, three regions of the traces were taken into consideration, the region before any bending event occurred (green), the region between any two bending events (blue), and the region after the last bending event (red). The distributions of the FRET states occupied in each region is plotted and shown with the corresponding color. **(F)** Cleavage of DF-50,1 and DF-60,1 occurs in an asynchronous manner after FEN1 enters the flow cell in contrast to DF-6,1. Distributions of the first time point of the bending step in each cleavage event were plotted for the different substrates (DF-6,1-cyan, DF-50,1-green and DF-60,1-purple). The data were fit to normal distributions and the means with standard deviation and N are reported. The mean and standard deviation values indicate broader distributions for DF-50,1 and DF-60,1 as compared to DF-6,1.

Supplementary Table 1. Kinetic parameters of FEN1 substrate bending and catalytic efficiency on DNA versus RNA EQ DF substrates.

	EQ DF-6,1		EQ DF-29,1	
	DNA	**RNA**	**DNA**	**RNA**
$K_{d\text{-}bending}$ (nM)	4.8 ± 0.6	32.1 ± 8.0	3.3 ± 0.4	103.0 ± 15.4
k_{on} ($\times 10^8$ M^{-1} s^{-1})	1.57 ± 0.47	0.58 ± 0.02	1.33 ± 0.01	0.39 ± 0.02
k_{off} (s^{-1})	0.45 ± 0.02	1.38 ± 0.02	0.37 ± 0.02	4.35 ± 0.04
$\tau_{bending\text{-}internal}$ (ms)	270 ± 70	160 ± 30	315 ± 65	220 ± 50
Missed cleavage events (%)	3.1	4.7	10.2	14.1

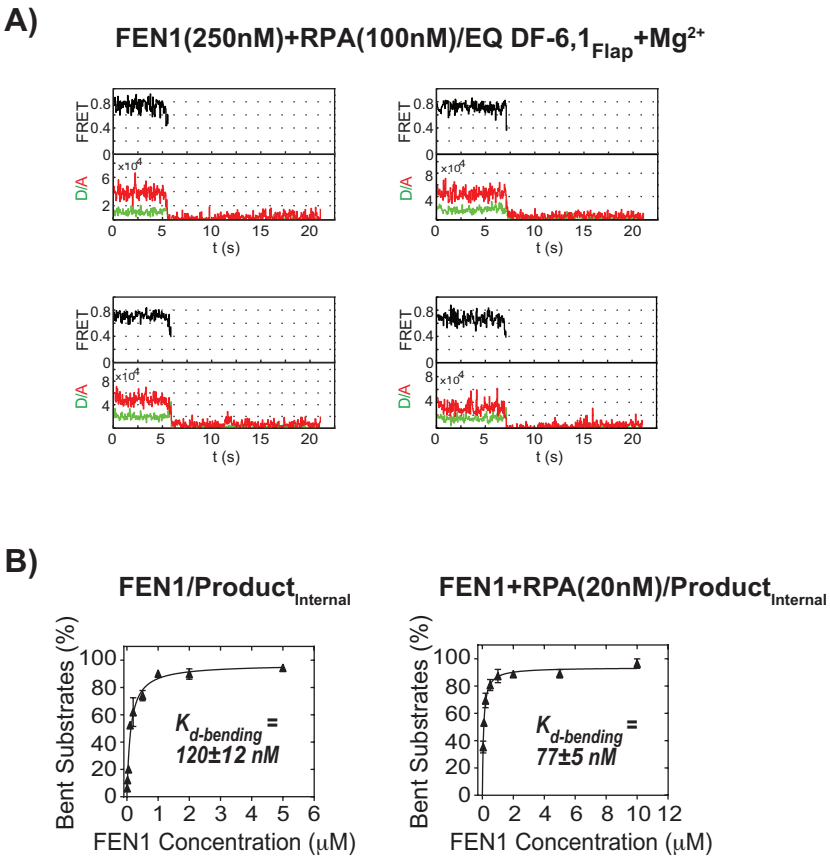

Supplementary Figure 4. (A) Representative time traces showing cleavage of EQ DF-6,1$_{Flap}$ in the presence of 100 nM RPA; FEN1 cleaves the substrate within first bending event as in Figure 7F. **(B)** FEN1 bending efficiency of Product$_{Internal}$ in the absence (left) and presence (right) of 20 nM RPA. Isotherms were obtained and fit as described for EQ DF-6,1$_{Internal}$ in Figure 2B. RPA does not display any significant effect on FEN1 bending efficiency with Product$_{Internal}$, and hence is unlikely to affect its product release kinetics.

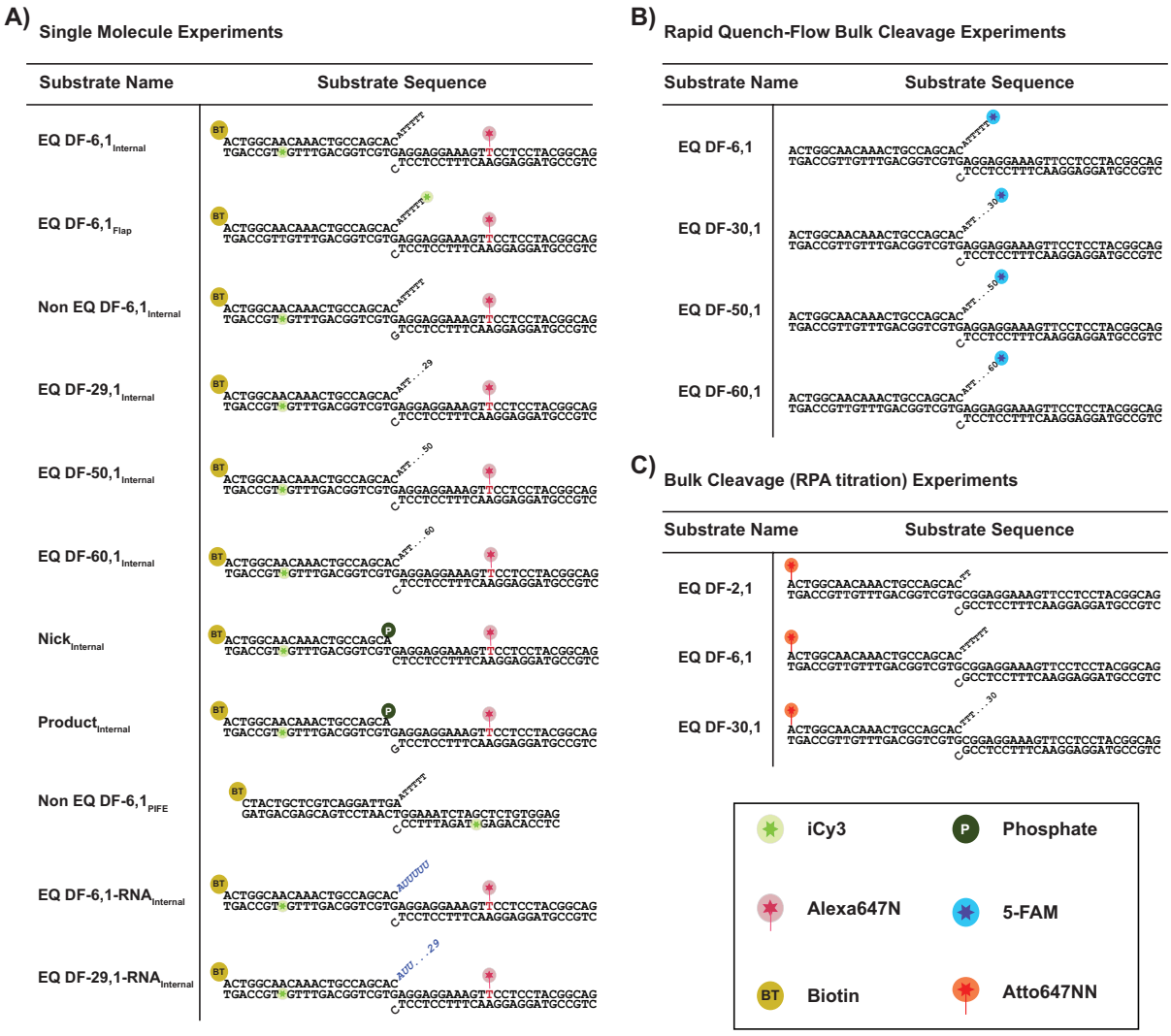

Supplementary Figure 5. Substrates used in this study. Schematic illustrating the sequences as well as modifications of the substrates used in this study. A legend of the symbols used is included. **(A)** Substrates used in single molecule bending and cleavage assays. **(B)** Substrates used in bulk stopped-flow single turnover and steady state cleavage assays. **(C)** Substrates used to assess RPA effect on FEN1 cleavage efficiency in bulk assays.